Molecular Therapy
Methods & Clinical Development
Original Article

A Long Intergenic Non-coding RNA, LINC01426, Promotes Cancer Progression via AZGP1 and Predicts Poor Prognosis in Patients with LUAD

Baorui Tian,[1,6] Xiaoyang Han,[1,6] Guanzhen Li,[2] Hua Jiang,[3] Jianni Qi,[4] Jiamei Li,[5] Yingying Tian,[1] and Chuanxi Wang[1,2]

[1]Department of Oncology, Shandong Provincial Hospital, Cheeloo College of Medicine, Shandong University, Jinan, Shandong, 250021, China; [2]Department of Oncology, Shandong Provincial Hospital Affiliated to Shandong First Medical University, Jinan, Shandong, 250021, China; [3]Department of Thoracic Surgery, Shandong Provincial Hospital Affiliated to Shandong First Medical University, Jinan, Shandong, 250021, China; [4]Department of Central Laboratory, Shandong Provincial Hospital Affiliated to Shandong First Medical University, Jinan, Shandong, 250021, China; [5]Department of Pathology, Shandong Provincial Hospital Affiliated to Shandong First Medical University, Jinan, Shandong, 250021, China

Various long non-coding RNAs (lncRNAs) are closely associated with lung adenocarcinoma (LUAD), playing oncogenic or anti-oncogenic roles in tumorigenesis and progression. Herein, we report a novel lncRNA—long intergenic non-protein coding RNA 1426 (LINC01426)—that has not yet been characterized in LUAD. We note that LINC01426 expression was markedly upregulated in LUAD tissues, and that functional assays verified that LINC01426 knockdown markedly inhibited cell proliferation, migration, and invasion *in vitro*. Xenografts derived from A549 cells knocked down of LINC01426 had evidently lower tumor weights and smaller tumor volumes. Our study also found that LINC01426 bound to hsa-miR-30b-3p as a competitive endogenous RNA in LUAD. Moreover, LINC01426 affected LUAD wound healing by interacting and combining with AZGP1, and LINC01426 expression was significantly associated with tumor-node-metastasis (TNM) staging and prognosis in patients with LUAD. To summarize, our study elucidates the oncogenic roles of LINC01426 in LUAD tumorigenesis and progression. We think that LINC01426 can serve as a potential diagnostic biomarker and therapeutic target in patients with LUAD.

INTRODUCTION

Lung cancer was the most frequently diagnosed cancer and the leading cause of cancer death among males in 2012 worldwide.[1] Moreover, in the United States, lung and bronchial cancer is the second common cancer and was the leading cause of cancer deaths in 2018.[2] According to the World Health Organization (WHO) classification, lung carcinomas can be divided into small-cell lung carcinoma and non-small-cell lung carcinoma (NSCLC). It is noteworthy that >85% of lung carcinoma-related deaths are currently attributable to NSCLC, for which the predicted 5-year survival rate is 15.9%. NSCLC can be subclassified into three major types: adenocarcinoma (50%), squamous cell carcinoma (~40%), and large cell carcinoma (~10%).[3] With regard to lung adenocarcinoma (LUAD), improvements have been made to facilitate its early diagnosis, and newly developed therapies are now available; however, the 5-year overall survival of patients with LUAD continues to remain low and the recurrence rate is still unsatisfactory.[4] Thus, identifying novel biomarkers for LUAD is critical for understanding the molecular alterations underlying this condition and for developing effective targeted therapies.

Although only <2% of human genome transcripts reportedly encode proteins, most nucleotides are detectably transcribed.[5] Among these nucleotides, long non-coding RNAs (lncRNAs) are a large class of non-protein-coding transcripts of >200 nt in length.[6] lncRNAs have emerged as important regulators, being involved in many physiological and pathological processes.[7] Assigning functions to lncRNAs depends on the development of high-throughput technologies, such as high-quality transcriptome annotations.[8] The human genome contains >60,000 lncRNAs,[7,9] and they play diverse roles in, for example, tumor migration and metastasis.[10] Although numerous lncRNAs reportedly have crucial functions in varied tumor processes, there are still many important lncRNAs that have not been reported or characterized. Thus, we need to elucidate the roles of lncRNAs in clinical therapy and/or disease diagnosis.

In the present study, using transcriptome sequencing analyses of four pairs of LUAD and adjacent normal lung tissues, we identified 18 genes with apparently abnormal changes in their expression. Subsequent screening by a high-content screening (HCS) proliferation assay led to the detection of long intergenic non-protein-coding RNA 1426

Received 15 July 2020; accepted 29 July 2020;
https://doi.org/10.1016/j.omtm.2020.08.001.

[6]These authors contributed equally to this work.

Correspondence: Chuanxi Wang, Department of Oncology, Shandong Provincial Hospital, Cheeloo College of Medicine, Shandong University, Jinan, Shandong, 250021, China
E-mail: chuanxiwang@126.com

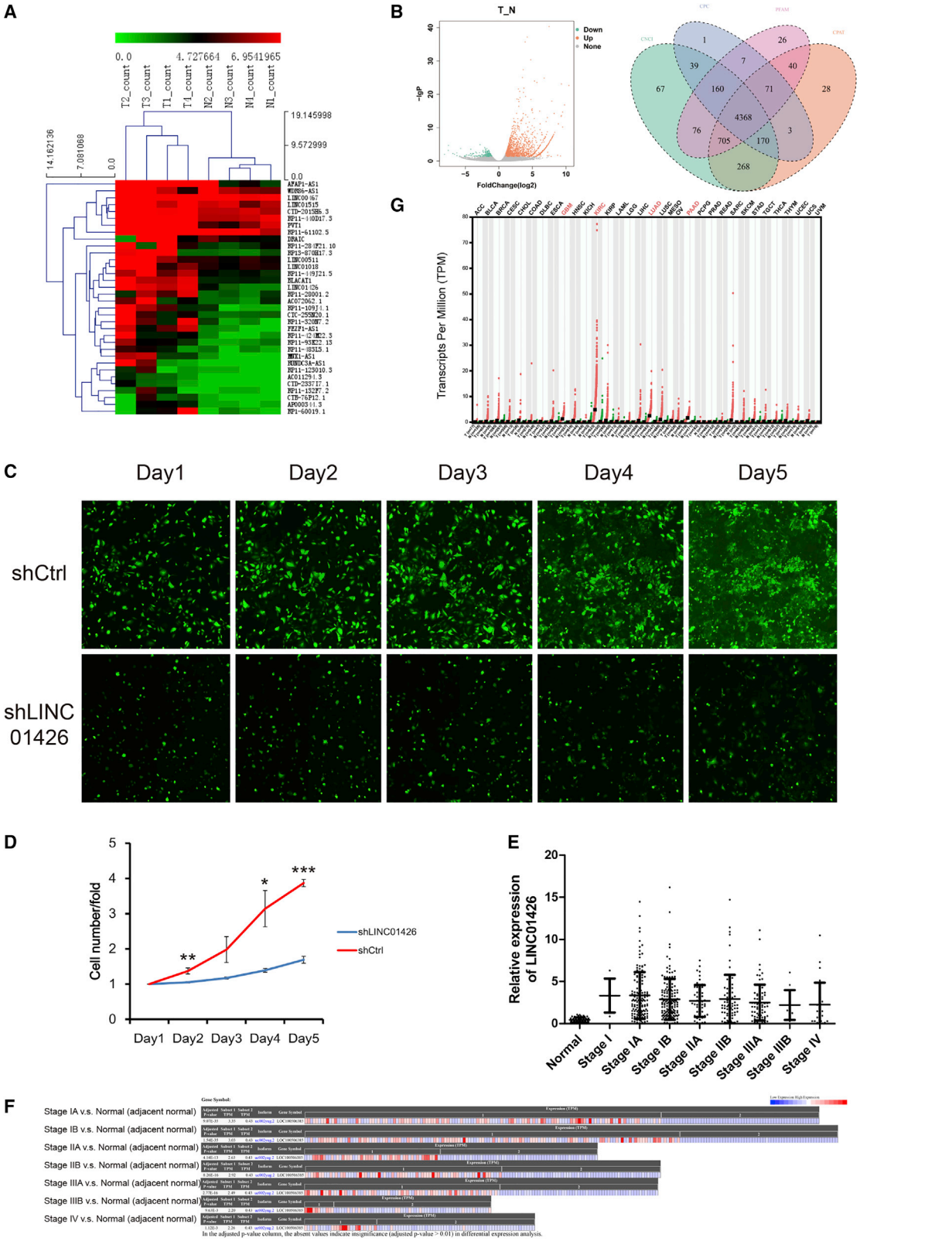

(legend on next page)

(LINC01426; ENST00000420877). We noted that LINC01426 markedly impacted cell proliferation; thus, we focused on understanding its role and the molecular mechanisms underlying its action in LUAD. LINC01426, also known as lincRNA-uc002yug.2, has been reported as a diagnostic marker for glioma[11] and esophageal cancer.[12] However, to date, no studies have reported the functions of LINC01426 in LUAD. In addition, there exists limited knowledge regarding the mechanism by which LINC01426 functions as an oncogenic lncRNA in LUAD and its diagnostic value.

Alpha-2-glycoprotein 1 (AZGP1) is a known tumor suppressor in hepatocellular carcinoma,[13,14] pancreatic cancer,[15] and colorectal cancer.[16] AZGP1 regulates cancer functions by regulating phosphatase and tensin homolog (PTEN) in hepatocellular carcinoma.[13] In this study, we identified a critical function of LINC01426 in LUAD: LINC01426 promoted the function of LUAD in A549 cells partly via *AZGP1*. We also found that LINC01426 bound to hsa-miR-30b-3p as a competitive endogenous RNA in LUAD. We report the clinical implications of LINC01426 in disease prognosis.

RESULTS

LINC01426 Is Highly Expressed in LUAD Tissues and May Be Associated with LUAD Functions

To investigate the expression of lncRNAs in LUAD, four pairs of LUAD and normal tissue samples were randomly selected for RNA sequence data analysis. As shown in Figures 1A and 1B, many more lncRNAs were differentially expressed in LUAD tissues than in normal tissues, including LINC01426 ($p < 0.01$). However, changes in gene expression levels do not imply that the respective genes have corresponding functions. Subsequently, 18 lncRNAs with significant changes in their expression were selected for HCS proliferation screening to identify lncRNAs that were significantly associated with LUAD functions. Our results showed that in A549 cells, transfection of shLINC01426 (knockdown of LINC01426) significantly decreased cell proliferation in comparison to transfection of shCtrl (corresponding negative control) (fold change ≥ 2.0), suggesting that LINC01426 is associated with LUAD functions (Figures 1C and 1D). Furthermore, analysis of the LUAD-associated RNA sequencing (RNA-seq) dataset based on The Cancer Genome Atlas (TCGA) using the bioinformatics tool Cancer RNA-seq Nexus[17] (http://syslab4.nchu.edu.tw/) showed that in comparison to normal tissues, LINC01426 was overexpressed in all stages in LUAD tissues ($p < 0.005$) (Figures 1E and 1F). Consistent with this finding, LINC01426 was also reported to be overexpressed in other types of tumors such as glioblastoma multiforme, renal clear cell carcinoma, and pancreatic adenocarcinoma by analyzing TCGA and Genotype-Tissue Expression (GTEx) data with GEPIA[18] ($p < 0.05$) (Figure 1G).

LINC01426 Knockdown Inhibits LUAD Proliferation *In Vitro*

To determine the biological role of LINC01426 in LUAD proliferation, A549 and NCI-H1299 cells were transfected with shLINC01426 and shCtrl. The effect of LINC01426 on cell proliferation was then detected using MTT (3-(4,5-dimethylthiazol-2-yl)-2,5-diphenyltetrazolium bromide; methyl thiazolyl tetrazolium) cell proliferation and clone formation assays, which indicated that upon LINC01426 knockout, cell proliferation and cell clone formation ability markedly decreased in both A549 and NCI-H1299 cells (Figures 2A–2C).

LINC01426 Inhibition Triggers LUAD Cell Apoptosis and Changes Cell Cycle Distribution *In Vitro*

Annexin V-allophycocyanin (APC) single-staining flow cytometry revealed that silencing LINC01426 in A549 and NCI-H1299 cells markedly increased cell apoptosis *in vitro* (Figures 3A and 3B); moreover, as indicated by propidium iodide (PI) staining flow cytometry, LINC01426 knockout significantly altered cell cycle distribution in both of the cell lines (Figures 3C and 3D).

LINC01426 Knockout Reduces Cell Invasion and Metastasis *In Vitro*

After corresponding lentivirus transfection in A549 and NCI-H1299 cells, wound healing migration and transwell migration assays were performed. Cell migration rates were significantly reduced in A549 and NCI-H1299 cells after LINC01426 knockdown (Figures 4A–4D). Furthermore, transwell invasion assay results showed that silencing LINC01426 inhibited LUAD metastasis in both of the cell lines (Figures 4E and 4F). These results suggested that LINC01426 reduces cell invasion and metastasis *in vitro*.

LINC01426 Knockdown Inhibits Tumor Proliferation *In Vivo*

A549 cells transfected with shLINC01426 and shCtrl were subcutaneously injected into nude mice. Images of sacrificed nude mice and tumors are shown in Figures 5A and 5C. Tumors derived from A549 cells transfected with shLINC01426 had significant lower weights and smaller volumes than did those derived from A549 cells transfected with shCtrl (Figures 5D and 5F). However, LINC01426 knockout had no significant effects on the body weight of mice (Figure 5B). Histological examinations using hematoxylin and eosin (H&E) staining demonstrated typical structures of LUAD to detect the success of adenocarcinoma formation (Figure 5E).

LINC01426 Directly Interacts with hsa-miR-30b-3p

In order to further explore the mechanism of LINC01426 in LUAD, through the comparison of original sequences, we found 13 binding bases in the conserved region of hsa-miR-30b-3p and LINC01426

Figure 1. LINC01426 Expression in LUAD and HCS Proliferation Assay

(A) Cluster analysis of representative lncRNAs. (B) Volcano map (left) and Venn diagram (right) upon sequencing of four lung adenocarcinoma (LUAD) and adjacent normal lung tissues. (C and D) HSC proliferation assay: (C) fluorescence images of A549 cells and (D) fold change in the number of A549 cells, as calculated by Celigo. (E) Relative expression of LINC01426 in different stages of LUAD and normal tissues based on TCGA data. (F) LINC01426 expression data based on TCGA were analyzed by Cancer RNA-seq Nexus. (G) LINC01426 expression in various cancers and adjacent normal lung tissues based on TCGA and GTEx data. shLINC01426, knockdown of LINC01426; shCtrl, corresponding negative control. All values are expressed as mean ± SD. *$p < 0.05$, **$p < 0.01$, ***$p < 0.001$.

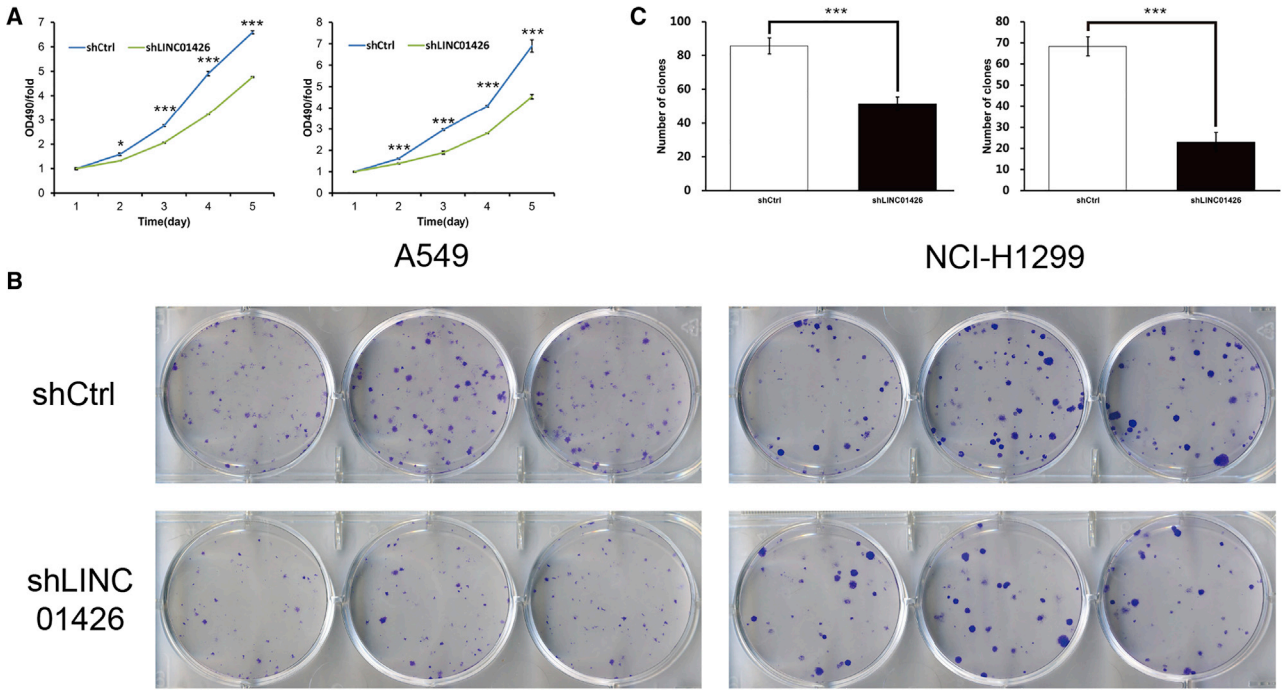

Figure 2. LINC01426 Knockdown Reduces LUAD Cell Proliferation and Cell Clone Formation *In Vitro*

(A) MTT assay was used to determine viability of A549 cells (left) and NCI-H1299 cells (right). (B) Representative images of colony formation assays using A549 and NCI-H1299 cells. (C) Number of clones in A549 (left) and NCI-H1299 (right) cells. shLINC01426, knockdown of LINC01426; shCtrl, corresponding negative control. All values are expressed as mean ± SD. *$p < 0.05$, **$p < 0.01$, ***$p < 0.001$.

(Figure 6A). It has been confirmed that the expression of hsa-miR-30b-3p is low in LUAD in previous studies and in the starBase database (Figure 6C), while the expression of LINC01426 is high in LUAD, so we speculated that LINC01426 directly interacted with hsa-miR-30b-3p. The luciferase results showed that hsa-miR-30b-3p mimics decreased the luciferase activity of PGL3-CMV-LUC-H_LINC01426 wild-type (WT) vector ($p < 0.01$) but had no markedly effect on that of the PGL3-CMV-LUC-H_LINC01426 mutant (MT) vector (Figure 6B). Taken together, we confirmed that there was a competitive binding between LINC01426 and hsa-miR-30b-3p. In addition, survival analysis of hsa-miR-30b-3p in LUAD was correlated with the LINC01426 we studied (Figure 6C).

Subcellular Localization of LINC01426

Localization of lncRNAs in cells is closely related to their mechanism of action. We thus used fluorescence *in situ* hybridization (FISH) to detect the subcellular localization of LINC01426. Confocal microscopy images showed that LINC01426 was mainly localized in the nucleus, and a small part of LINC01426 was also located in the cytoplasm along the nuclear membrane (Figure 7A).

LINC01426 Affects LUAD Wound Healing by Interacting and Combining with *AZGP1*

Molecules that may interact with LINC01426 were screened using RNA pull-down assays and mass spectrometry (Figure 7B). KEGG and Gene Ontology (GO) analyses of the screened proteins using ClueGO[19] and CluePedia[20] are shown in Figure 7C. In addition, transcriptome analysis was performed using RNA obtained from A549 cells that were transfected with shLINC01426 or shCtrl (Figure 7D). Furthermore, we identified the direct interaction of AZGP1 and LINC01426 by RNA pulldown (Figure 7E). Also, KEGG and GO analyses of differentially expressed gene using ClueGO[19] and CluePedia[20] are shown in Figure 7F. We found that *AZGP1* combined with LINC01426; moreover, 23 differentially expressed genes after LINC01426 knockdown were associated with the phosphatidylinositol 3-kinase (PI3K)/AKT pathway, which was determined to interact with AZGP1.[13] Therefore, we suspect that AZGP1 interacts with LINC01426. Furthermore, to confirm the role of AZGP1 in LINC01426-inhibited LUAD migration, we transfected lvAZGP1 (overexpressed AZGP1) to LINC01426 knockdown A549 cells. After calculating the average mobility and its variation between groups in three replicates, results verified that inhibition of tumor migration in A549 cells by LINC01426 knockdown was enhanced in the context of AZGP1 overexpression compared with A549 cells transfected with shCtrl (Figure 7G). However, qRT-PCR confirmed no significant change in LINC01426 expression with the overexpression of AZGP1, whereas no significant change in AZGP1 expression with the knockdown of LINC01426 (data not shown). Consistently, western blot showed that LINC01426 expression did not correlate with *AZGP1* expression (Figure 7H). Interestingly, LINC01426 expression, normalized by GAPDH, was positively correlated with AZGP1 and PTEN expression normalized by GAPDH based on TCGA using GEPIA[18]

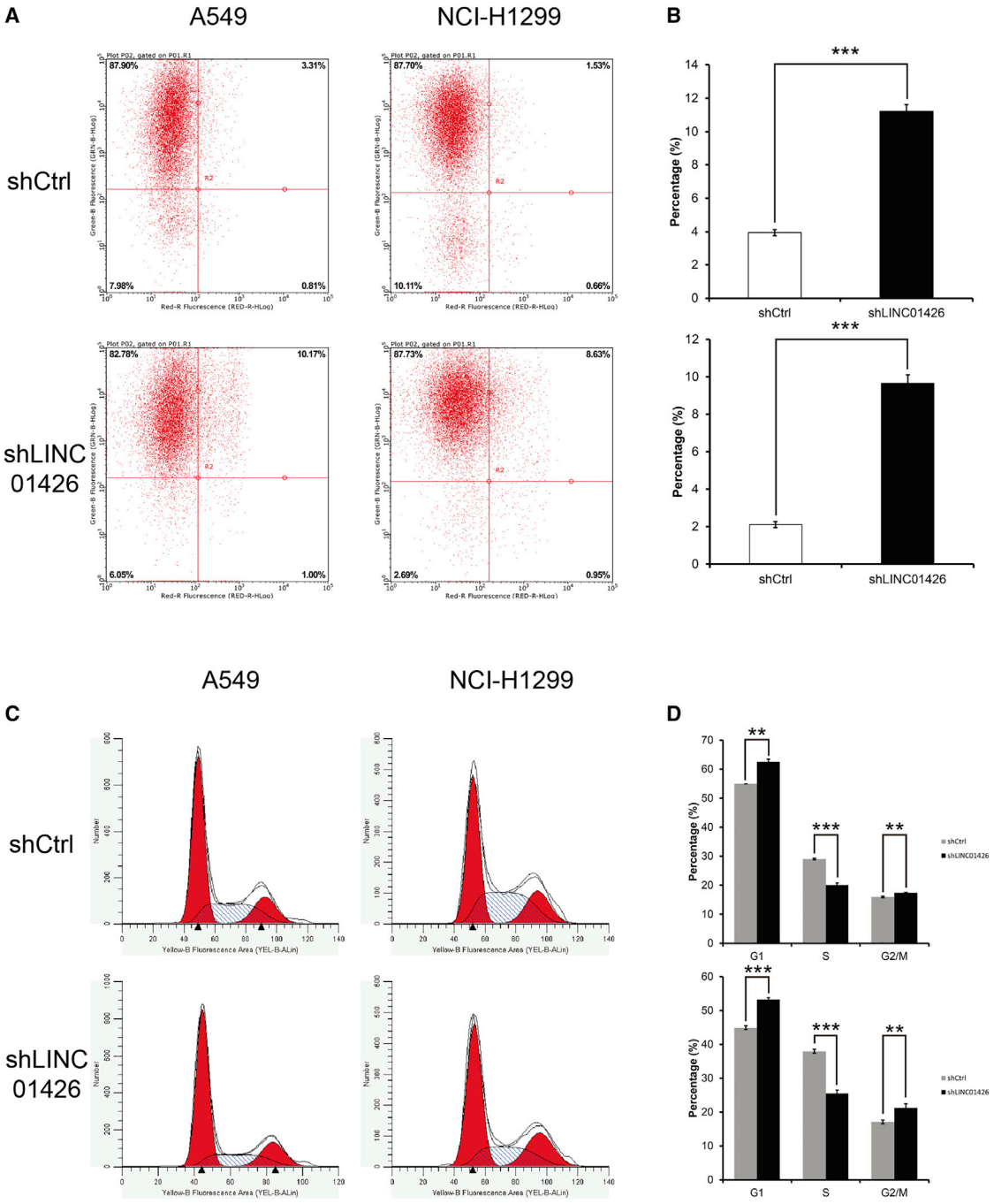

Figure 3. LINC01426 Knockdown Promotes Cell Proliferation and Changes Cell Cycle Distribution *In Vitro*

(A) Flow cytometric analysis of apoptosis in A549 and NCI-H1299 cells. (B) Percentage of apoptosis in A549 (upper) and NCI-H1299 (lower) cells. (C) Flow cytometric analysis of cell cycle distribution in A549 and NCI-H1299 cells. (D) Distribution of cell cycle in A549 (upper) and NCI-H1299 (lower) cells. shLINC01426, knockdown of LINC01426; shCtrl, corresponding negative control. All values are expressed as mean ± SD. *$p < 0.05$, **$p < 0.01$, ***$p < 0.001$.

(Figure 7I). Therefore, we think that LINC01426 inhibits the function of *AZGP1* specifically; LINC01426 thus promotes LUAD progression partly via antagonizing with *AZGP1*. This in turn somewhat explains why AZGP1 expression is not a prognostic marker for lung cancer.[21]

LINC01426 Expression Is Significantly Correlated with Prognosis and TNM Staging

LUAD and normal tissue samples were subjected to FISH and H&E staining (Figure 8A). The results of t tests showed that LINC01426

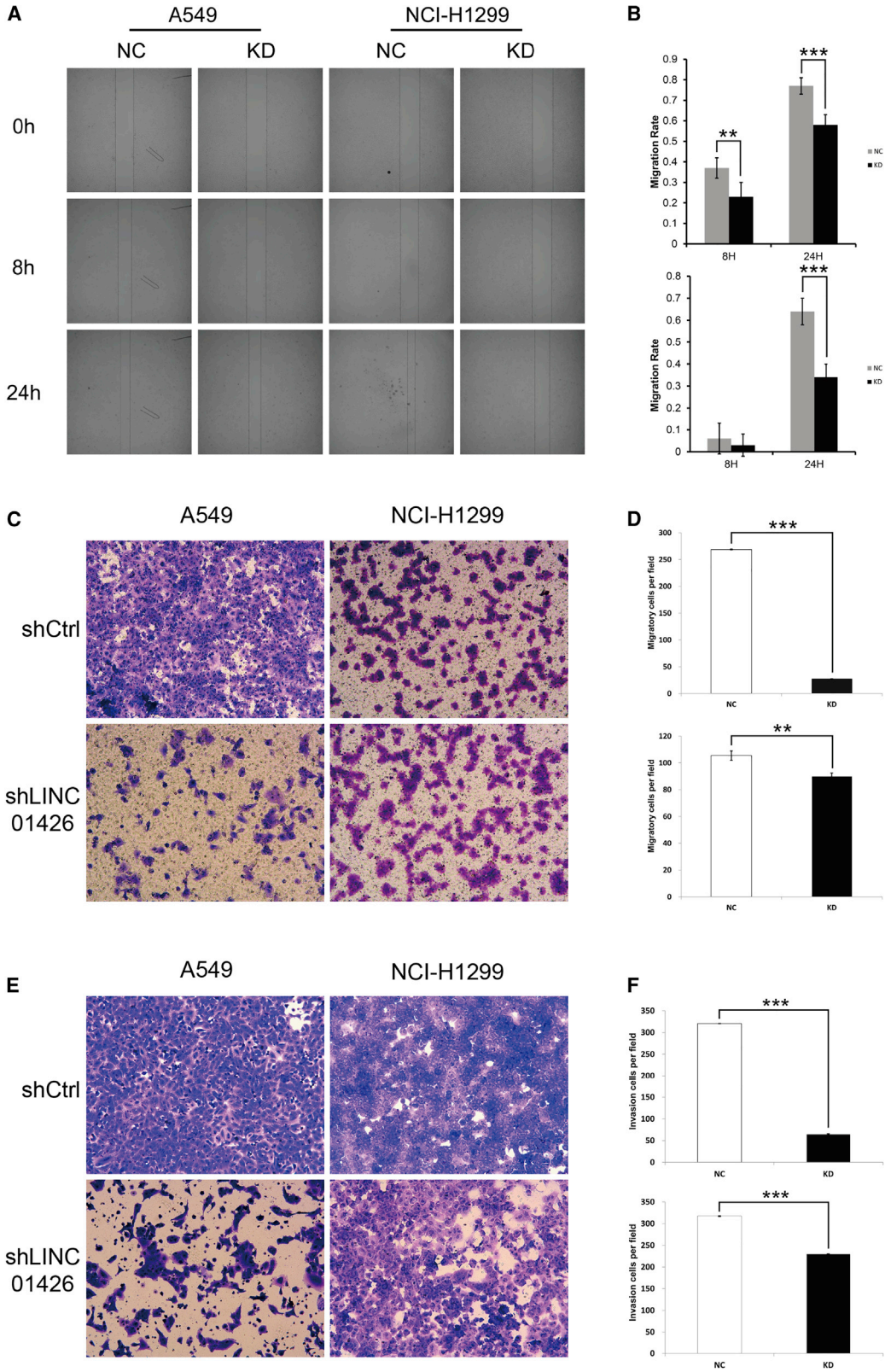

(legend on next page)

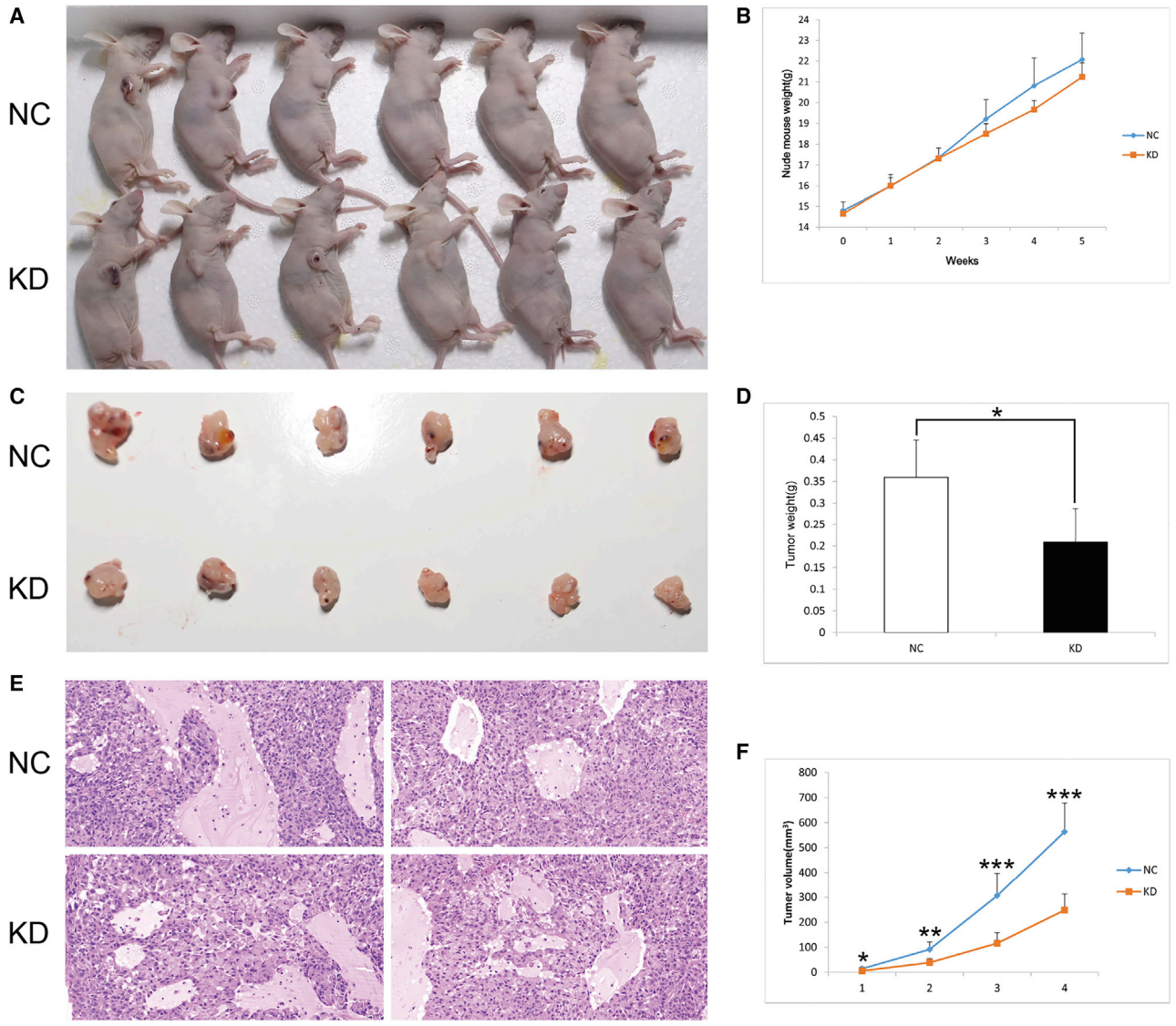

Figure 5. LINC01426 Downregulation Suppresses LUAD Tumor Growth *In Vivo*

(A) Sacrificed nude mice with xenograft tumor. (B) Nude mice weight curve. (C) Images of tumors collected from mice. (D) Tumor weight curve. (E) Representative images upon H&E staining of tumor sections. (F) Tumor volume curve. KD, knockdown of LINC01426; NC, corresponding negative control. All values are expressed as mean ± SD. *p < 0.05, **p < 0.01, and ***p < 0.001. All values are expressed as mean ± SD.

was differentially expressed both in the nucleus and cytoplasm in LUAD and normal tissues (p < 0.001) (Table1). A chi-square test and Spearman analysis indicated that LINC01426 expression both in the nucleus and cytoplasm was associated with tumor-node-metastasis (TNM) staging (p < 0.005), N staging (p < 0.005), and EGFR expression (p < 0.05) in LUAD; furthermore, LINC01426 expression in the nucleus was associated with LUAD T stage (p < 0.05) (Tables 2 and 3). In addition, analysis of the LUAD-associated RNA-seq dataset based on TCGA showed that LINC01426 mRNA expression levels were higher in stage II/III/IV patients than in stage I (p < 0.01) (Figure 8B). Kaplan-Meier analysis and log-rank test results showed that the expression of LINC01426 both in the nucleus and cytoplasm was

Figure 4. LINC01426 Knockdown Inhibits Cell Migration and Invasion *In Vitro*

(A) Representative images of wound healing assays at indicated times after scratching A549 and NCI-H1299 cells. (B) Migration rate at indicated times in A549 and NCI-H1299 cells. (C) Representative images of transwell migration assays in A549 and NCI-H1299 cells. (D) Migratory cells per field in A549 and NCI-H1299 cells. (E) Representative images of transwell invasion assays in A549 and NCI-H1299 cells. (F) Invasion cells per field in A549 and NCI-H1299 cells. shLINC01426, knockdown of LINC01426; shCtrl, corresponding negative control. All values are expressed as mean ± SD. *p < 0.05, **p < 0.01, ***p < 0.001.

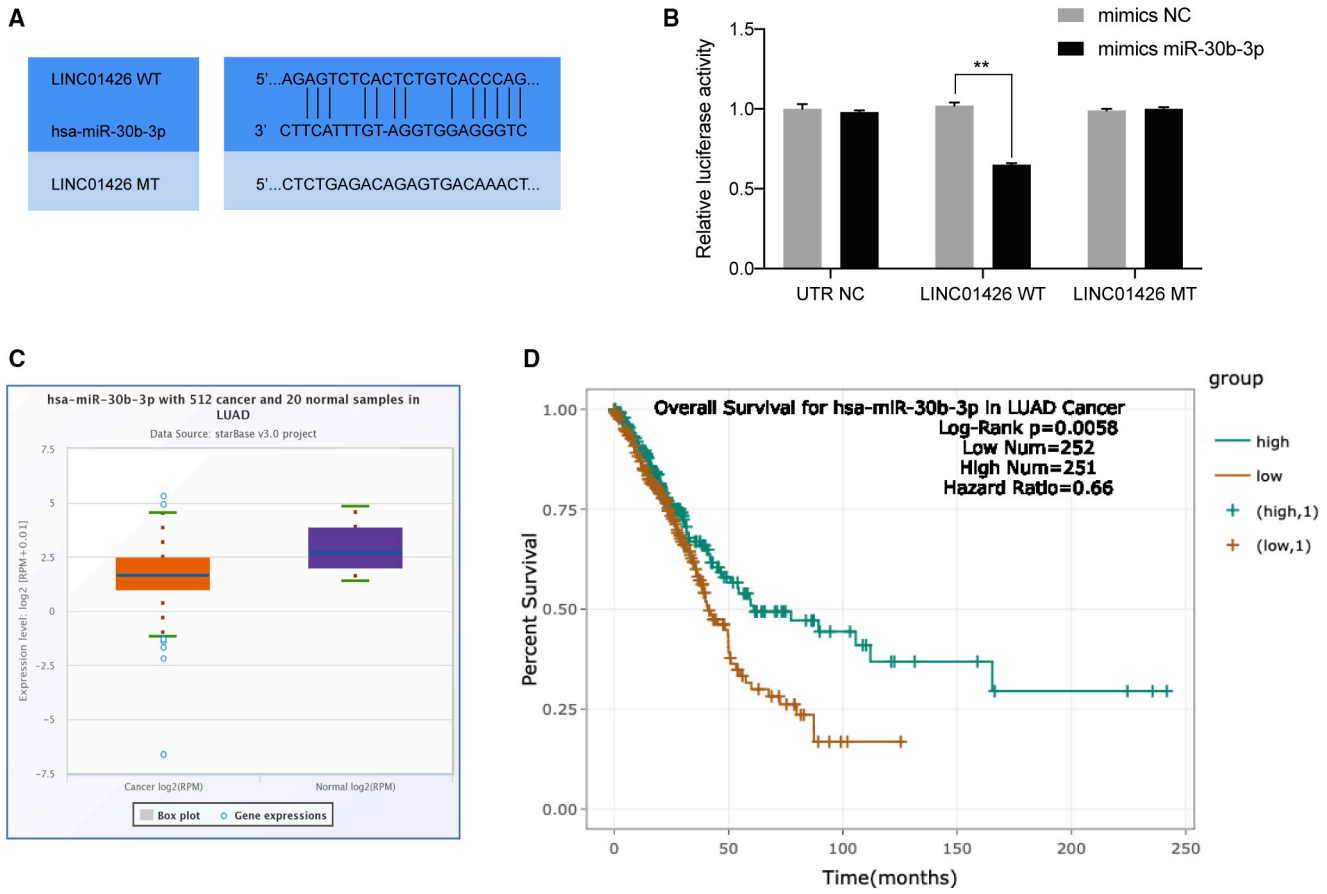

Figure 6. LINC01426 Directly Interacts with hsa-miR-30b-3p

(A) Binding bases in the conserved region of LINC01426 and hsa-miR-30b-3p. (B) Luciferase reporter assay results showed that hsa-miR-30b-3p mimics decreased the luciferase activity of the PGL3-CMV-LUC-H_LINC01426 WT vector ($p < 0.01$). (C) The expression of hsa-miR-30b-3p in cancer tissues was lower than in normal tissues in LUAD ($p<0.05$). (D) The expression of hsa-miR-30b-3p in LUAD and its association with overall survival in LUAD (data are from starBase [https://bio.tools/starbase]).

associated with overall survival of patients with LUAD ($p < 0.05$); grouping was based on the multiplication of "staining intensity score" and "staining positive rate score" (Figure 8C). However, COX multivariate regression analysis showed that expression of LINC01426 was not an independent predictor of patients with LUAD (data not shown). Results indicated that LINC01426 expression was significantly associated with TNM staging and prognosis in patients with LUAD.

DISCUSSION

An increasing number of recent studies have reported that lncRNAs play an important role in cancers;[22,23] also, the lncRNA-related database has gradually improved with technological advancements.[24] Many lncRNAs such as LINC00312[25] and CAR10[26] reportedly affect a variety of LUAD functions such as proliferation, invasion, apoptosis, and metastasis. By exploring the mechanisms underlying the action of lncRNAs, we may be better able to understand carcinogenesis and cancer progression in patients with LUAD. In addition, although the clinical application of lncRNAs remains scarce, they have the potential to become a diagnostic and prognostic marker and a therapeutic target in patients with LUAD.[27,28] Therefore, in this study, we attempted to identify an LUAD-related lncRNA and explore its potential as a diagnostic and prognostic marker.

We used LUAD and normal tissue samples to identify differentially expressed lncRNAs. LINC01426 was selected for further studies considering its significant overexpression in LUAD and its dramatic effect on cell proliferation. LINC01426 is a oncogene and its function has been reported in glioma[11] and esophageal cancer,[12] but no studies have yet been conducted to explore the effect of LINC01426 on LUAD functions and mechanisms. Our results indicated that LINC01426 knockout inhibited LUAD proliferation, increased cell apoptosis, and affected cell cycle distribution *in vitro*. LINC01426 knockdown had a similar effect on tumor growth *in vivo*. Furthermore, knocking out LINC01426 inhibited the migration and invasiveness abilities of LUAD cells *in vitro*. LINC01426 thus seems to have a complicated connection with LUAD carcinogenesis and progression.

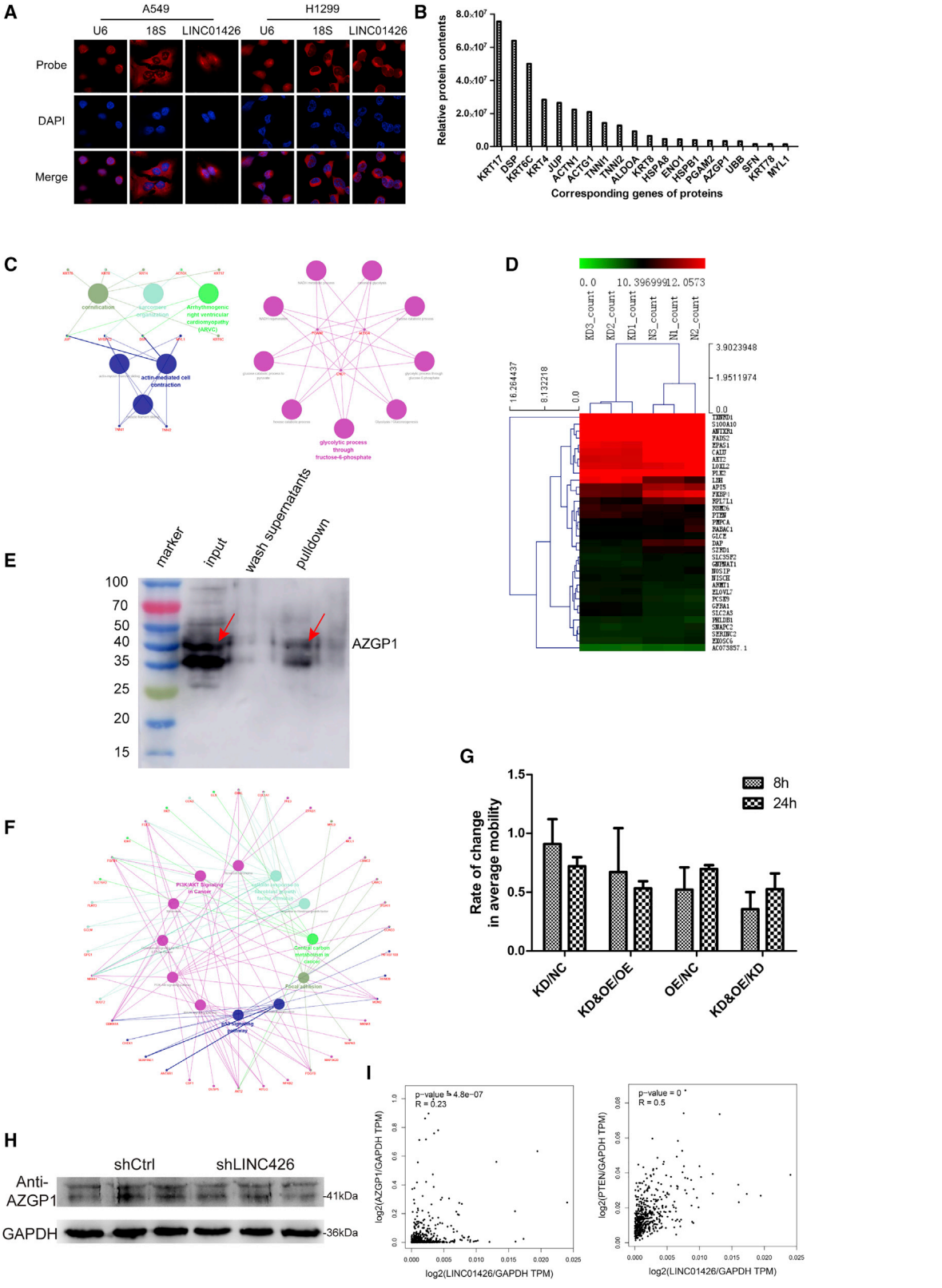

(legend on next page)

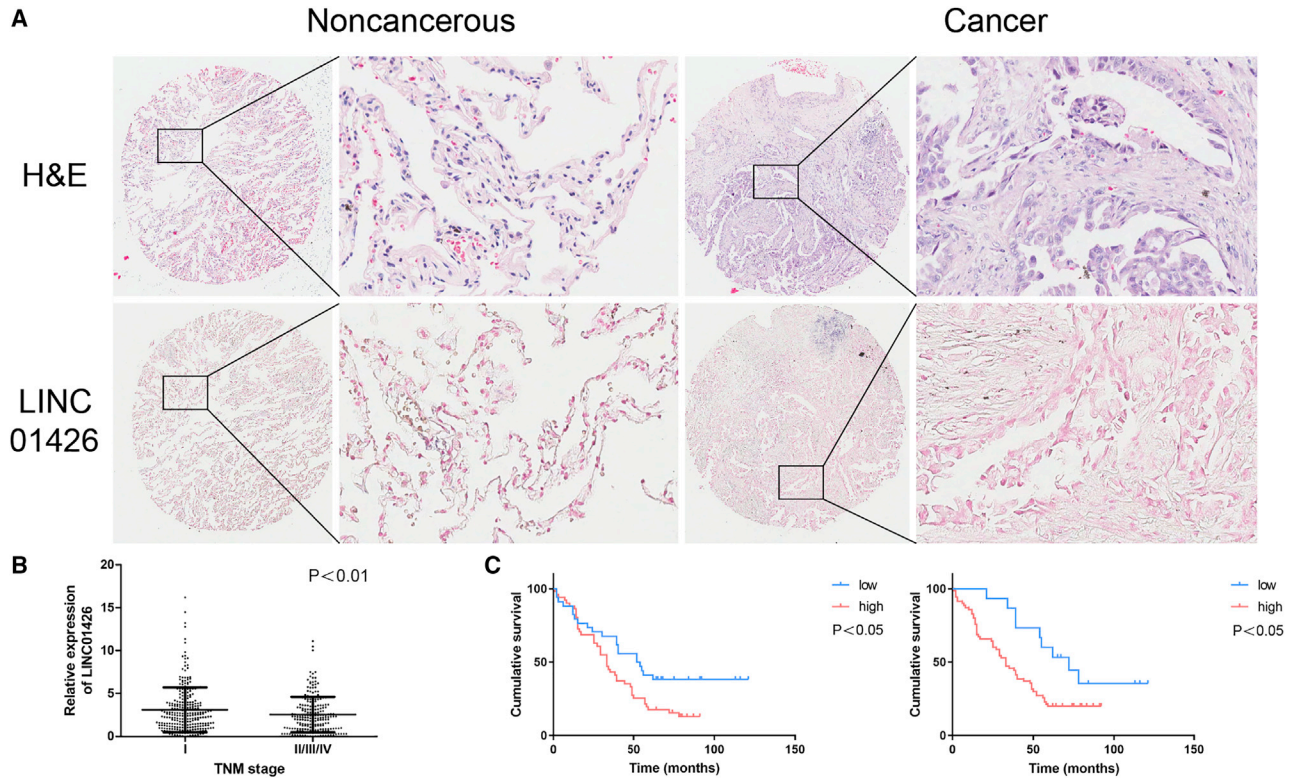

Figure 8. Prognostic Value of the Expression of LINC01426 in Patients with LUAD

(A) ISH (LINC01426) and H&E staining of LUAD and adjacent normal lung tissues. (B) The association of LINC01426 expression with TNM stage in LUAD tissues. (C) Kaplan-Meier analysis showing that LINC01426 expression in the nucleus (left) and cytoplasm (right) was associated with overall survival of patients with LUAD. All values are expressed as mean ± SD.

AZGP1 is a known tumor suppressor gene in hepatocellular carcinoma,[13,14] pancreatic cancer,[15] and colorectal cancer.[16] AZGP1 has the potential to be used as the predictor of cancers such as prostate cancer,[29] gastric cancer,[30] and breast cancer;[31] moreover, AZGP1 autoantibody and mRNA levels in normal human lung tissues can reportedly help predict lung cancer prognosis.[21,32] However, no significant differences have been reported in the content of AZGP1 between different diagnosis or clinical stage in LUAD,[32] and the cause for this observation remains to be clearly explained. AZGP1 has also been confirmed to affect tumor progression via PTEN in hepatocellular carcinoma,[13] and AZGP1 expression is associated with PTEN-deleted prostate cancers.[33] In this study, *AZGP1* was one of the proteins that combined with LINC01426 screened by us using an RNA pull-down assay. Transcriptome sequencing results confirmed that LINC01426 was associated with the PI3K/AKT pathway, which interacts with AZGP1 reportedly.[13] With the results of functional experiments, we speculate that LINC01426 affects LUAD progression via *AZGP1*. Considering the high expression of LINC01426 and the low expression of AZGP1 in LUAD, shLINC01426 and lvAZGP1 are used in this study. However, our research cannot explain why LINC01426 expression is positively correlated with AZGP1 and PTEN expression in LUAD. Further studies need to be conducted to explore whether other genes also combine and interact with LINC01426 and also to verify the relationship between LIANC01426 and AZGP1.

Recently, lncRNAs such as CAR10,[26] MUC5B-AS1,[34] and CASC2[35] have been reported to be associated with prognosis in patients with LUAD. The high expression of LINC01426 in the nucleus and cytoplasm was verified to be significantly associated with poor prognosis. Furthermore, the expression of LINC01426 in the nucleus and

Figure 7. LINC01426 Is Mainly Located in the Nucleus and Interacts with *AZGP1*

(A) Confocal microscopy images. (B) Mass spectrometry results of RNA pull-down. (C) KEGG and GO analysis of mass spectrometry results. (D) Cluster analysis of A549 cells transfected with shLINC01426 and shCtrl. (E) RNA pull-down results showed that LINC01426 binds to AZGP1. (F) KEGG and GO analysis of sequencing results. (G) Rate of change in average mobility of A549 cells transfected with different lentiviruses. (H) The expression of AZGP1 was detected by western blotting in A549 cells transfected with shLINC01426 and shCtrl. (I) Correlation analysis of mRNA expression of LINC01426 and AZGP1 (left)/PTEN (right) normalized by GAPDH based on TCGA. KD, knockdown of LINC01426; OE, overexpression of AZGP1; NC, corresponding negative control; shLINC01426, knockdown of LINC01426; shCtrl, corresponding negative control. All values are expressed as mean ± SD. *p < 0.05, **p < 0.01, ***p < 0.001.

Table 1. Differential Expression of LINC01426 between LUAD and Lung Tissues

	n	LINC01426 Expression		Chi-Square Value	p Value
		High (%)	Low (%)		
LUAD (cytoplasm)	86	66	20	41.112	0.000*
Lung tissues (cytoplasm)	86	24	62		
LUAD (nucleus)	86	47	39	57.790	0.000*
Lung tissues (nucleus)	86	2	84		

*$p < 0.05$ (statistically significant).

cytoplasm was associated with both LUAD TNM and N staging. These findings highlight the significance of LINC01426 as an attractive candidate biomarker for the diagnosis and prognosis of LUAD.

In conclusion, we report that LINC01426 combines with *AZGP1* to influence LUAD functions. LINC01426 overexpression was significantly associated with poor prognosis in patients with LUAD. Also, LINC01426 binds to miR-30b-3p as a competitive endogenous RNA in LUAD. Moreover, it has the potential to be a valuable biomarker and therapeutic target in LUAD. Further studies on the mechanisms underlying and clinical validation of LINC01426 are warranted.

MATERIALS AND METHODS

Tissue Samples and Clinical Data Collection

From July 2004 to June 2009, 86 pairs of LUAD and adjacent normal lung tissue samples were collected from patients who had undergone surgery at Provincial Hospital Affiliated to Shandong University. Through follow-up until August 2014, complete prognostic information could be obtained for 85 pairs of samples. Histopathological examination was used to confirm LUAD, and no patients underwent chemotherapy or radiotherapy preoperatively. Patient-related information was obtained via medical records, and LUAD clinical stage was determined based on the TNM classification system.[36] The study was approved by the Committees for Ethical Review of Research involving Human Subjects at Provincial Hospital Affiliated to Shandong University. Written informed consent was obtained from all patients. All samples were stored at −80°C until further use.

Cell Culture

Two LUAD cell lines, A549 and NCI-H1299, were obtained from ScienCell (San Diego, CA, USA). A549 and NCI-H1299 cells were cultured in F-12K (Gibco, Grand Island, NY, USA) and RPMI 1640 (Gibco) media, respectively. Both media were supplemented with 10% fetal bovine serum (Gibco), 100 μg/mL penicillin (Sigma, St. Louis, MO, USA), and 100 μg/mL streptomycin (Sigma). The cells were maintained at 37°C in a 5% CO_2-enriched humidified air atmosphere.

RNA Isolation, Reverse Transcription, PCR, and Quantitative Real-Time PCR

Total RNA was extracted from cells and tissues using RNAiso Plus (TaKaRa, Dalian, China) according to the manufacturer's instructions. For qRT-PCR, cDNA was synthesized using a PrimeScript RT reagent kit (TaKaRa), and the reaction was performed using a PCR machine (Thermo Fisher Scientific, CA, USA). To detect gene expression levels, quantitative real-time PCR was performed on a Roche LightCycler 480 (Roche, Shanghai, China) using a TB Green Premix Ex Taq II kit (TaKaRa). For amplifying cDNA sequences, cDNA was synthesized with specific primer sequences using a PrimeScript RT reagent kit (TaKaRa), and PCR was performed using PrimeSTAR Max DNA polymerase (TaKaRa) on a PCR machine (Thermo Fisher Scientific). GAPDH primer, obtained from TaKaRa, was used as the internal control. The primer sequences are as follows: LINC01426 primers for quantitative real-time PCR, forward, 5′-CAGCTTGCTTAGTTGCAGTGTTTC-3′, reverse, 5′-ATCATG GTAAGATGACCAGGTTGAC-3′; AZGP1 primers for quantitative real-time PCR, forward, 5′-CACTGGGCTGTCCAAGCAT-3′, reverse, 5′-CTCCATTCCTTCCACCTGTCTC-3′; PTEN primers for quantitative real-time PCR, forward, 5′-AGCGTGCAGATAA TGACAAGGA-3′, reverse, 5′-GATTTGACGGCTCCTCTACTG TTT-3′; LINC01426 primers for PCR, forward, 5′-TAATACGACT CACTATAGGGAGACTGTGAACGTGACCAGACCT-3′, reverse, 5′-TCTTGGCTCACTGCAACCTC-3′; LINC01426 primers for RT, forward, 5′-GGAAATGGAATGAGACT-3′, reverse, 5′-CTCCAT CAGTCTCTTTTG-3′. Relative fold changes in expression were calculated using the $2^{-\Delta\Delta CT}$ method.

RNA Sequence Data Analysis

The integrity and concentration of the extracted total RNA were determined using an Agilent 2100 RNA Nano 6000 assay kit (Agilent Technologies, CA, USA). rRNAs were removed using a Ribo-Zero Gold kit (Illumina, CA, USA). lncRNA libraries were built with NEBNext Ultra directional RNA library prep kit (Illumina). The constructed libraries were used for Illumina sequencing, and the sequencing error rate was calculated based on the Phred score.

Cell Transfection

The recombinant lentivirus of LINC01426 knockout (shLINC01426), AZGP1 overexpression (lvAZGP1), and corresponding negative control (shCtrl) were designed and synthesized by GeneChem (Shanghai, China). To increase transfection efficiency, we used 4% HitransG A (GeneChem). The efficiency of transfection was assessed after 48 h according to the expression of green fluorescent protein, and cells were screened by puromycin. qRT-PCR was performed to detect knockout efficiency in the first application of each lentivirus; the recombinant lentivirus was qualified when the knockout efficiency was <70%.

HCS Proliferation Assay

Recombinant lentivirus-transfected cells were seeded in 96-well cell culture plates at 37°C. The number of cells with green fluorescence signals was calculated by a Celigo imaging cytometer (Nexcelom, Beijing, China). Cell proliferation status was determined using a growth curve, which plotted the number of cells measured on 5 consecutive days.

Table 2. Correlation between LINC01426 Expression and Clinicopathological Characteristics in the Cytoplasm

		LINC01426 Expression				
	Variables	Low	High	Total	Chi-Square Value	p Value
Age (years)					0.001	0.975
	≤60	10	33	43		
	>60	12	39	51		
T stage					4.08	0.043*
	T1/T2	20	50	70		
	T3/T4	2	22	24		
Sex					0.039	0.843
	female	10	31	41		
	male	12	41	53		
TNM stage					12.3	0*
	I/II	19	30	49		
	III/IV	1	29	30		
	null					
N stage					15.9	0*
	N0	19	23	42		
	N1/N2/N3	2	35	37		
	null					
M					0.295	0.587
	M0	21	71	92		
	M1	0	1	1		
	null					
VEGF					0.652	0.42
	negative	11	29	40		
	positive	11	43	54		
	null					
Grade					1.91	0.167
	I/II	17	50	67		
	III	3	22	25		
PD-L1					0.765	0.382
	negative	3	8	11		
	positive	12	61	73		
	null					
Survivin					0.094	0.759
	negative	3	10	13		
	positive	11	46	57		
	null					
ALK					1	0.316
	negative	12	59	71		
	positive	2	4	6		
	null					
EGFR					3.91	0.048*
	negative	15	51	66		
	positive	0	14	14		
	null					

*$p < 0.05$ (statistically significant).

Table 3. Correlation between LINC01426 Expression and Clinicopathological Characteristics in the Nucleus

		LINC01426 Expression				
	Variables	Low	High	Total	Chi-Square Value	p Value
Age (years)					0.937	0.333
	≤60	22	21	43		
	>60	21	30	51		
T stage					3.56	0.059
	T1/T2	36	34	70		
	T3/T4	7	17	24		
Sex					0.537	0.464
	female	17	24	41		
	male	26	27	53		
TNM stage					10.7	0.001*
	I/II	30	19	49		
	III/IV	7	23	30		
	null					
N stage					17.7	0*
	N0	29	13	42		
	N1/N2/N3	8	29	37		
	null					
M					0.832	0.362
	M0	42	50	92		
	M1	0	1	1		
	null					
VEGF					0.086	0.769
	negative	19	21	40		
	positive	24	30	54		
	null					
Grade					0.164	0.686
	I/II	29	38	67		
	III	12	13	25		
PD-L1					3.14	0.076
	negative	7	4	11		
	positive	26	47	73		
	null					
Survivin					0.567	0.452
	negative	4	9	13		
	positive	24	33	57		
	null					
ALK					0.13	0.719
	negative	29	42	71		
	positive	2	4	6		
	null					
EGFR					5.52	0.019*
	negative	32	34	66		
	positive	2	12	14		
	null					

*$p < 0.05$ (statistically significant).

MTT Cell Proliferation Assay

Cells were cultivated in 96-well plates at 37°C and transfected with recombinant lentivirus. Subsequently, from the second to the sixth day, 20 μL of 5 mg/mL MTT (Genview, Beijing, China) was added to one well per group, and culture was terminated after 4 h, without changing the culture medium. Then, 100 μL of DMSO (MP Biomedicals, CA, USA) was added to solubilize formazan crystals, followed by oscillation for 2–5 min. Optical density at 490/570 nm was measured using a microplate reader (Tecan Infinite, Switzerland). Each experiment was repeated three times.

Cell Clone Formation Assay

Cells were seeded at a density of 500 cells/well in six-well cell culture plates at 37°C for 14 days. After taking photographs and washing with phosphate-buffered saline (PBS; Solarbio, Baijing, China), the cells were fixed for 30 min by adding 1 mL of 4% paraformaldehyde (Solarbio) to each well. Subsequently, the fixed cells were stained for 15 min using 500 μL of Giemsa stain (Solarbio). Then, photographs were taken with a digital camera (Sony, Tokyo, Japan) and clones were counted.

Flow Cytometry

Post-transfected A549 and NCI-H1299 cells were washed with cold PBS (Solarbio) three times. To analyze cell apoptosis, the cells were centrifuged and subsequently stained using an annexin V-APC apoptosis detection kit (eBioscience, Shanghai, China) according to the manufacturer's instructions. The cells were then analyzed using a FlowSight imaging flow cytometer (Millipore, Shanghai, China), and data analysis was performed using CellQuest software (Millipore). The relative ratios of apoptotic cells were compared with control transfection. For cell cycle analysis, the cells are fixed in 75% alcohol for 1 h; subsequently, the fixed cells were washed with PBS (Solarbio) and stained with PI (Sigma, Shanghai, China). The cells were analyzed by a FlowSight imaging flow cytometer (Millipore), and the percentages of cells in the G_0/G_1, S, or G_2/M phase were counted and compared. All samples were assayed in triplicates.

Wound Healing Migration Assay

The cells in the cell culture plates were scratched using a scratcher or 200-μL pipette tips. The cells were then lightly rinsed using serum-free medium two to three times and cultured in serum-free medium. Photographs were taken at 0, 8, and 24 h to calculate the wound healing migration rate.

Transwell Migration and Invasion Assays

We performed transwell assays to measure cell invasion and migration rates. Transwell assays were carried out using 24-well plates with BD BioCoat Matrigel chambers (8-μm pores; BD Biosciences, USA). For migration assays, a total of 1×10^5 A549 or NCI-H1299 cells/well were seeded in the upper chamber and cultured in the serum-free medium, whereas 1×10^5 cells were added to the upper chamber pre-coated with 1:8 diluted Matrigel (BD Biosciences) for invasion assays. Medium with 30% serum was placed in the lower chambers. After incubation for 24 h, cells were fixed with 4% paraformaldehyde (Solarbio) for 0.5 h and stained with 0.5% of crystal violet (Solarbio) for 5 min. Invasive cells on the lower surface of the membrane were counted at ×200 magnification by a microscope.

Western Blot

Cells were washed twice with PBS (Solarbio). Total protein was extracted from the cell lines using radioimmunoprecipitation assay (RIPA) buffer (Beyotime, Shanghai, China) supplemented with 1% phenylmethylsulfonyl fluoride (Thermo Fisher Scientific), and protein concentrations were determined using a bicinchoninic acid (BCA) protein assay kit (Beyotime). Then, equal amounts of protein samples were separated by sodium dodecyl sulfate polyacrylamide gel electrophoresis and transferred onto polyvinylidene fluoride membranes (Millipore). Subsequently, the membrane was blocked with 5% nonfat milk and probed with primary antibodies, followed by incubation overnight at 4°C. Then, secondary antibodies (Beyotime) were applied. GAPDH was used as the loading control. All of the primary antibodies were from Abcam. Protein bands were analyzed using the Immobilon western chemiluminescent horseradish peroxidase (HRP) substrate (Millipore) and an imaging system (Bio-Rad, CA, USA). All experiments were performed at least three times.

Luciferase Reporter Assay

The WT and MUT LINC01426 were constructed into PGL3-CMV-LUC-LINC01426 WT and PGL3-CMV-LUC-LINC01426 MT (Genomeditech, Shanghai, China) respectively. The plasmid was prepared by a high-purity plasmid extraction kit (QIAGEN), and then the plasmid constructed by 100-ng and 30 nM mimics miR-30b-3p/mimics NC vector (Genomeditech, Shanghai, China) were cotransfected into HEK293 cells. The cells were lysed by cell lysis buffer after 48 h. The luciferase activity and Renilla luciferase activity were continuously detected by a luciferase analysis system (Genomeditech) and a Centro XS3 LB 960 multifunctional microplate reader (Berthold Technologies). Relative luciferase activity was normalized with Renilla luciferase activity.

FISH

Probe sets for LINC01426, U6 (nuclear), and 18S (cytoplasmic) controls were synthesized by RiboBio Technology (Guangzhou, China). The assay was performed using a FISH kit (RiboBio) according to the manufacturer's instructions.

RNA Pull-Down Assay

First, to synthesize monoclonal RNA sequences, antisense DNA templates with the T7 RNA polymerase promoter site upstream of the sequence were synthesized by performing RT-PCR with specific primers. Next, antisense DNA templates were purified using a PureLink quick PCR purification combo kit (Invitrogen, CA, USA) and transcribed into monoclonal RNA sequences using a MEGAscript kit (Invitrogen). The RNA-binding protein was then obtained with a Pierce magnetic RNA-protein pull-down kit (Thermo Fisher Scientific) and identified by mass spectrometry performed by the Beijing

Institute of Animal Husbandry and Veterinary. All protocols were performed as per the manufacturers' instructions.

Tumor-Bearing Nude Mice Model

Five-week-old male BALB/c nude mice were subcutaneously injected with 2×10^6 transfected A549 cells. Animal weight and tumor volume were recorded every week. After 35 days, the animals were sacrificed and tumor weight was measured. Tumors were analyzed by H&E staining and partially stored at −80°C for subsequent experiments. All animal experiments were approved by the Animal Care and Use Committee at Provincial Hospital Affiliated to Shandong University.

Statistical Analysis

Values are presented as mean ± SD. We used a t test to compare differences and a one-way analysis of variance (ANOVA) to compare mean values among groups. A chi-square test and Spearman analysis were used to analyze the associations between LINC01426 expression and the clinicopathological variables. Survival was estimated with the Kaplan-Meier (log rank) method and independent predictors with COX multivariate regression analysis. SPSS 17.0 was used for data analyses; $p < 0.05$ indicated statistical significance.

AUTHOR CONTRIBUTIONS

Conceptualization, C.W.; Methodology, B.T. and X.H.; Investigation, X.H. and H.J; Writing, B.T. and X.H.; Funding Acquisition and Supervision, C.W.; Resources, G.L., J.Q., and J.L.

CONFLICTS OF INTEREST

The authors declare no competing interests.

ACKNOWLEDGMENTS

This study was supported by the National Natural Science Foundation of China (81473483), the Natural Science Foundation of Shandong Province (BS2013YY048, 2016GSF201139, 201603029), the China Postdoctoral Science Foundation (2015M572056), and by a grant provided by Jinan City (201620169). We thank Shizhe Liu for technical support.

REFERENCES

1. Torre, L.A., Bray, F., Siegel, R.L., Ferlay, J., Lortet-Tieulent, J., and Jemal, A. (2015). Global cancer statistics, 2012. CA Cancer J. Clin. *65*, 87–108.
2. Siegel, R.L., Miller, K.D., and Jemal, A. (2018). Cancer statistics, 2018. CA Cancer J. Clin. *68*, 7–30.
3. Chen, Z., Fillmore, C.M., Hammerman, P.S., Kim, C.F., and Wong, K.K. (2014). Non-small-cell lung cancers: a heterogeneous set of diseases. Nat. Rev. Cancer *14*, 535–546.
4. Martin, P., and Leighl, N.B. (2017). Review of the use of pretest probability for molecular testing in non-small cell lung cancer and overview of new mutations that may affect clinical practice. Ther. Adv. Med. Oncol. *9*, 405–414.
5. Djebali, S., Davis, C.A., Merkel, A., Dobin, A., Lassmann, T., Mortazavi, A., Tanzer, A., Lagarde, J., Lin, W., Schlesinger, F., et al. (2012). Landscape of transcription in human cells. Nature *489*, 101–108.
6. Ponting, C.P., Oliver, P.L., and Reik, W. (2009). Evolution and functions of long noncoding RNAs. Cell *136*, 629–641.
7. Iyer, M.K., Niknafs, Y.S., Malik, R., Singhal, U., Sahu, A., Hosono, Y., Barrette, T.R., Prensner, J.R., Evans, J.R., Zhao, S., et al. (2015). The landscape of long noncoding RNAs in the human transcriptome. Nat. Genet. *47*, 199–208.
8. Lagarde, J., Uszczynska-Ratajczak, B., Carbonell, S., Pérez-Lluch, S., Abad, A., Davis, C., Gingeras, T.R., Frankish, A., Harrow, J., Guigo, R., and Johnson, R. (2017). High-throughput annotation of full-length long noncoding RNAs with capture long-read sequencing. Nat. Genet. *49*, 1731–1740.
9. Chen, Y.G., and Chang, H.Y. (2017). lncRNA seduction of GOT2 goes viral. Immunity *47*, 1021–1023.
10. Dhamija, S., and Diederichs, S. (2016). From junk to master regulators of invasion: lncRNA functions in migration, EMT and metastasis. Int. J. Cancer *139*, 269–280.
11. Wang, S.J., Wang, H., Zhao, C.D., and Li, R. (2018). Long noncoding RNA LINC01426 promotes glioma progression through PI3K/AKT signaling pathway and serves as a prognostic biomarker. Eur. Rev. Med. Pharmacol. Sci. *22*, 6358–6368.
12. Wu, H., Zheng, J., Deng, J., Zhang, L., Li, N., Li, W., Li, F., Lu, J., and Zhou, Y. (2015). *LincRNA-uc002yug.2* involves in alternative splicing of *RUNX1* and serves as a predictor for esophageal cancer and prognosis. Oncogene *34*, 4723–4734.
13. Tian, H., Ge, C., Zhao, F., Zhu, M., Zhang, L., Huo, Q., Li, H., Chen, T., Xie, H., Cui, Y., et al. (2017). Downregulation of AZGP1 by Ikaros and histone deacetylase promotes tumor progression through the PTEN/Akt and CD44s pathways in hepatocellular carcinoma. Carcinogenesis *38*, 207–217.
14. Xu, M.Y., Chen, R., Yu, J.X., Liu, T., Qu, Y., and Lu, L.G. (2016). AZGP1 suppresses epithelial-to-mesenchymal transition and hepatic carcinogenesis by blocking TGFβ1-ERK2 pathways. Cancer Lett. *374*, 241–249.
15. Kong, B., Michalski, C.W., Hong, X., Valkovskaya, N., Rieder, S., Abiatari, I., Streit, S., Erkan, M., Esposito, I., Friess, H., and Kleeff, J. (2010). AZGP1 is a tumor suppressor in pancreatic cancer inducing mesenchymal-to-epithelial transdifferentiation by inhibiting TGF-β-mediated ERK signaling. Oncogene *29*, 5146–5158.
16. Chang, L., Tian, X., Lu, Y., Jia, M., Wu, P., and Huang, P. (2019). Retracted. PLoS ONE *14*, e0215712.
17. Li, J.R., Sun, C.H., Li, W., Chao, R.F., Huang, C.C., Zhou, X.J., and Liu, C.C. (2016). Cancer RNA-Seq Nexus: a database of phenotype-specific transcriptome profiling in cancer cells. Nucleic Acids Res. *44* (D1), D944–D951.
18. Tang, Z., Li, C., Kang, B., Gao, G., Li, C., and Zhang, Z. (2017). GEPIA: a web server for cancer and normal gene expression profiling and interactive analyses. Nucleic Acids Res. *45* (W1), W98–W102.
19. Bindea, G., Mlecnik, B., Hackl, H., Charoentong, P., Tosolini, M., Kirilovsky, A., Fridman, W.H., Pagès, F., Trajanoski, Z., and Galon, J. (2009). ClueGO: a Cytoscape plug-in to decipher functionally grouped gene ontology and pathway annotation networks. Bioinformatics *25*, 1091–1093.
20. Bindea, G., Galon, J., and Mlecnik, B. (2013). CluePedia Cytoscape plugin: pathway insights using integrated experimental and in silico data. Bioinformatics *29*, 661–663.
21. Albertus, D.L., Seder, C.W., Chen, G., Wang, X., Hartojo, W., Lin, L., Silvers, A., Thomas, D.G., Giordano, T.J., Chang, A.C., et al. (2008). AZGP1 autoantibody predicts survival and histone deacetylase inhibitors increase expression in lung adenocarcinoma. J. Thorac. Oncol. *3*, 1236–1244.
22. Bhan, A., Soleimani, M., and Mandal, S.S. (2017). Long noncoding RNA and cancer: a new paradigm. Cancer Res. *77*, 3965–3981.
23. Huarte, M. (2015). The emerging role of lncRNAs in cancer. Nat. Med. *21*, 1253–1261.
24. Gao, Y., Wang, P., Wang, Y., Ma, X., Zhi, H., Zhou, D., Li, X., Fang, Y., Shen, W., Xu, Y., et al. (2019). Lnc2Cancer v2.0: updated database of experimentally supported long non-coding RNAs in human cancers. Nucleic Acids Res. *47* (D1), D1028–D1033.
25. Peng, Z., Wang, J., Shan, B., Li, B., Peng, W., Dong, Y., Shi, W., Zhao, W., He, D., Duan, M., et al. (2018). The long noncoding RNA LINC00312 induces lung adenocarcinoma migration and vasculogenic mimicry through directly binding YBX1. Mol. Cancer *17*, 167.
26. Ge, X., Li, G.Y., Jiang, L., Jia, L., Zhang, Z., Li, X., Wang, R., Zhou, M., Zhou, Y., Zeng, Z., et al. (2019). Long noncoding RNA CAR10 promotes lung adenocarcinoma metastasis via miR-203/30/SNAI axis. Oncogene *38*, 3061–3076.
27. Kumar, P., Khadirnaikar, S., and Shukla, S.K. (2019). A novel lncRNA-based prognostic score reveals TP53-dependent subtype of lung adenocarcinoma with poor survival. J. Cell. Physiol. *234*, 16021–16031.

28. Liao, M., Liu, Q., Li, B., Liao, W., Xie, W., and Zhang, Y. (2018). A group of long non-coding RNAs identified by data mining can predict the prognosis of lung adenocarcinoma. Cancer Sci. *109*, 4033–4044.

29. Henshall, S.M., Horvath, L.G., Quinn, D.I., Eggleton, S.A., Grygiel, J.J., Stricker, P.D., Biankin, A.V., Kench, J.G., and Sutherland, R.L. (2006). Zinc-alpha2-glycoprotein expression as a predictor of metastatic prostate cancer following radical prostatectomy. J. Natl. Cancer Inst. *98*, 1420–1424.

30. Huang, C.Y., Zhao, J.J., Lv, L., Chen, Y.B., Li, Y.F., Jiang, S.S., Wang, W., Pan, K., Zheng, Y., Zhao, B.W., et al. (2013). Decreased expression of AZGP1 is associated with poor prognosis in primary gastric cancer. PLoS ONE *8*, e69155.

31. Stavnes, H.T., Nymoen, D.A., Langerød, A., Holth, A., Børresen Dale, A.-L., and Davidson, B. (2013). *AZGP1* and *SPDEF* mRNA expression differentiates breast carcinoma from ovarian serous carcinoma. Virchows Arch. *462*, 163–173.

32. Falvella, F.S., Spinola, M., Pignatiello, C., Noci, S., Conti, B., Pastorino, U., Carbone, A., and Dragani, T.A. (2008). AZGP1 mRNA levels in normal human lung tissue correlate with lung cancer disease status. Oncogene *27*, 1650–1656.

33. Burdelski, C., Kleinhans, S., Kluth, M., Hube-Magg, C., Minner, S., Koop, C., Graefen, M., Heinzer, H., Tsourlakis, M.C., Wilczak, W., et al. (2016). Reduced AZGP1 expression is an independent predictor of early PSA recurrence and associated with ERG-fusion positive and *PTEN* deleted prostate cancers. Int. J. Cancer *138*, 1199–1206.

34. Yuan, S., Liu, Q., Hu, Z., Zhou, Z., Wang, G., Li, C., Xie, W., Meng, G., Xiang, Y., Wu, N., et al. (2018). Long non-coding RNA MUC5B-AS1 promotes metastasis through mutually regulating MUC5B expression in lung adenocarcinoma. Cell Death Dis. *9*, 450.

35. Wang, D., Gao, Z.M., Han, L.G., Xu, F., Liu, K., and Shen, Y. (2017). Long non-coding RNA CASC2 inhibits metastasis and epithelial to mesenchymal transition of lung adenocarcinoma via suppressing SOX4. Eur. Rev. Med. Pharmacol. Sci. *21*, 4584–4590.

36. Sobin, L.H., Gospodarowicz, M., and Wittekind, C. (2010). TNM Classification of Malignant Tumours, Seventh Edition (Wiley-Blackwell).